Linking water vapor sorption to water repellency in soils with high organic carbon contents

Hermansen, Cecilie; Norgaard, Trine; de Jonge, Lis Wollesen; Weber, Peter L.; Moldrup, Per; Greve, Mogens H.; Tuller, Markus; Arthur, Emmanuel

Published in:
Soil Science Society of America Journal

DOI (link to publication from Publisher):
10.1002/saj2.20248

Publication date:
2021

Document Version
Accepted author manuscript, peer reviewed version

Linking water vapor sorption to water repellency in soils with high organic carbon contents

Cecilie Hermansen[a*], Trine Norgaard[a], Lis Wollesen de Jonge[a], Peter L. Weber[a], Per Moldrup[b], Mogens H. Greve[a], Markus Tuller[c], and Emmanuel Arthur[a]

[a]Dept. of Agroecology, Faculty of Technical Sciences, Aarhus University, Blichers Allé 20, DK-8830 Tjele, Denmark

[b]Dept. of the Built Environment, Faculty of Engineering and Science, Aalborg University, Thomas Manns Vej 23, DK-9220 Aalborg Ø, Denmark

[c]Dept. of Environmental Science, The University of Arizona, 1177 E. 4th Street, Tucson, Arizona 85721, USA

*Corresponding author e-mail address: Cecilie.hermansen@agro.au.dk

Core ideas (3 to 5 statements of 85 characters or less):

1. Water vapor sorption isotherms (WSIs) of high organic soils were hysteretic
2. Magnitude of water sorption consistently increased with organic carbon (OC) content
3. The area below water repellency curves (WRC) increased with OC content
4. WSI parameters estimated WRC parameters with a higher accuracy than OC content
5. WSI models accurately estimated WRC from hygroscopic water contents at arbitrary RH

Abbreviations:

C_a and C_d, energy constants for adsorption and desorption; CL, clay content; GAB, Guggenheim, Anderson, and de Boer; *Hys*, hysteresis; K_a and K_d, model parameters for adsorption and desorption; MED, molarity of an ethanol droplet; MLR, multiple linear regression; OC, organic carbon; OM, organic matter; *r*, Pearson correlation coefficient; RH, relative humidity; RMSE, root mean square error; *w,* water content; $w_{m\text{-}a}$ and $w_{m\text{-}d,}$ the monolayer *w* from adsorption and desorption isotherms, respectively; w_{non}, critical water content; WR, water repellency; WR_{area}, total soil water repellency; WSI, water vapor sorption isotherm; w_{50a} and w_{50d}, the soil *w* at 50% *RH* for adsorption and desorption, respectively.

This article has been accepted for publication and undergone full peer review but has not been through the copyediting, typesetting, pagination and proofreading process, which may lead to differences between this version and the Version of Record. Please cite this article as doi: 10.1002/saj2.20248.

Abstract

Water repellency (WR) significantly affects the hydraulic behavior of soils. Although WR often is regarded as a phenomenon with implications for dry soils, it is prevalent at water contents (*w*) exceeding the wilting point water content. Because the measurement of the WR–*w* relationship is laborious, alternative more time-efficient methods are desirable to estimate parameters of the WR-*w* curve. Using 32 high organic soils from Denmark and South Greenland, we characterized the water vapor sorption isotherms (WSIs), investigated the interrelated effects of organic carbon (OC) and clay contents on WSIs and the WR–*w* relationship, and further evaluated if parameters of the WR-*w* curve may be derived directly from WSIs. The samples exhibited OC and clay contents ranging from 0.014 to 0.369 kg kg^{-1} and 0.02 to 0.16 kg kg^{-1}, respectively. The WSIs measured for relative humidity (*RH*) values between 3 and 93%, were strongly hysteretic, OC dependent, and could be accurately characterized with the Guggenheim, Anderson, and de Boer (GAB) model. Further, the WR_{area} and w_{non} parameters, derived from WR measured for several *w*, were well estimated with linear regressions based on OC content and multiple linear regressions based on OC and clay contents. Estimations for WR_{area} and w_{non} based on the WSI parameter $w_{m\text{-}a}$ were superior to OC and clay content. Finally, we established mathematical expressions that estimate WR_{area} or w_{non} from any air-dry *w* obtained from either the desorption or adsorption isotherms between 10 and 90% RH.

Keywords:
Molarity of an ethanol droplet method, Vapor sorption analyzer, Hysteresis, Critical water content, Hydrophobicity

1. Introduction

Soil water repellency (WR) is predominant at many locations across the world. Extensive WR surveys across New Zealand, South Greenland, Wales, and Western Australia discovered hydrophobic or potentially hydrophobic soils at more than 90% of the studied sites (Harper and Gilkes, 1994; Deurer et al., 2011; Hermansen et al., 2019; Seaton et al., 2019; Weber et al., 2021). Moreover, WR is prevalent across other countries, such as China, Africa, and the USA (DeBano, 1981; Scott, 2000; Ruwanza and Shackleton, 2016; Gao et al., 2018; Chen et al., 2020). Soil water repellency can decrease infiltration (Leighton-Boyce et al., 2007; Müller et al., 2010), increase overland flow and thus surface erosion (Osborn et al., 1964; Leighton-Boyce et al., 2007), and further initiate localized flow events in soils that are typically not prone to fast preferential flow phenomena (Doerr et al., 2000; de Jonge et al., 2009). Although WR can have adverse implications for plant growth and increase the transport of contaminants to groundwater, the initiation of WR in soils might be a response to external environmental stress from soil biota (Seaton et al., 2019).

Considering the prevalence of WR and its effects on hydrological processes, assessment of WR should be part of routine soil analyses. However, measurements of WR are very laborious, which often hinders a thorough evaluation of WR prevalence. Due to the nonlinear WR dependency on soil water content (*w*), it is required to measure the magnitude of WR across a wide range of *w* to obtain a full characterization of total soil WR, i.e. the trapezoidal integrated area under the soil water repellency characteristic curve (WR_{area}) (de Jonge et al., 1999; de Jonge et al., 2007; Kawamoto et al.,

2007). Further, a critical point at the WR-*w* curve (w_{non}) defines a threshold below which WR varies nonlinearly with *w*, and above which the soil remains hydrophilic (de Jonge et al., 1999). To improve agricultural irrigation practices, knowledge of w_{non} could be beneficial for remediation of WR (Hermansen et al., 2019). The WR dependency on *w* emanates from the orientation of functional groups in organic matter. At low *w*, polar functional groups of OM are directed inwards, thus exposing hydrophobic ends, rendering the soil water repellent. As *w* increases, functional groups of OM reorient and increasingly expose hydrophilic functional groups (Mas'shum and Farmer, 1985; Doerr et al., 2000). Knowledge of the total amount of OC in a soil sample may be used to estimate WR_{area} and w_{non} (de Jonge et al., 1999; Karunarathna et al., 2010; Hermansen et al., 2019). It has recently been suggested that equations based on OC and clay can provide even better estimates of w_{non} for subarctic soils (Weber et al., 2021).

Soil water vapor sorption isotherms (WSIs) relate the relative vapor pressure or water activity to soil *w* for matric potentials smaller than −10 MPa (relative humidity, RH < 95%), where adsorptive forces dominate soil water retention (Tuller and Or, 2005; Davis et al., 2009). Several studies (e.g., Arthur et al., 2016, 2020; Lu and Khorshidi, 2015) have shown that the WSIs for the majority of soils are hysteretic (larger *w* for desorption than for adsorption). The extent of hysteresis depends on the OC and clay contents as well as clay mineralogy. Soils with high OC and clay contents, and smectite-rich soils tend to be more hysteretic (Arthur et al., 2020). There is a potential link between WSIs and WR for soils as shown in Arthur et al. (2014) and Weber et al. (2020). The latter study indicates that the slope of the water potential (pF 6.9 to 3) gravimetric soil *w* relationship correlates linearly with WR_{area} and w_{non} (Weber et al., 2021).

Proper management of natural and agricultural organic matter rich soils is crucial for the mitigation of adverse impacts of WR on the environment, such as the deterioration of ground and surface water quality due to increased surface runoff and enhanced preferential transport of contaminants. Direct WR measurements across a wide range of water contents are time-consuming, WSIs can be rapidly measured with an automated vapor sorption analyzer (Arthur et al., 2014). This provides an opportunity to link soil water sorption and WR and further quantify the magnitude of WR based on WSIs as suggested by Arthur et al. (2014). When WSIs and WR are successfully linked, it is feasible to estimate WR based on a single measure of hygroscopic water content, within the RH range of the measured WSIs. Further, since OC content affects both the magnitude of WR and the water vapor sorption hysteresis, it is interesting to investigate if the OC content serves as a link between WSIs and the defining parameters of the WR–*w* relationship (WR_{area} and w_{non}) for organic matter rich soils. Thus, the overall aim of this paper was to answer the following questions for organic matter rich soils obtained from Denmark and South Greenland:

- How are parameters derived from water vapor sorption isotherms related to OC and clay content?
- How are the soil water repellency parameters, WR_{area} and w_{non}, linked to OC and clay contents, and the parameters derived from water vapor sorption isotherms?
- Is it feasible to obtain the WR_{area} and w_{non} parameters directly from one soil water content measurement?

2. Materials & Methods

2.1 Investigated soil samples

A total of 32 soil samples were investigated – 20 from a field in Obakker, Denmark, and 12 from several sites in South Greenland. The 20 soil samples from Obakker were collected from the topsoil across a field of 4.5 ha in 2015 (depth from 5 to 20 cm). The soil samples from South Greenland were extracted from eight agricultural fields from 2015 to 2018. The soils were sampled below the thatch layer from approximately 5 to 15 cm depths. Detailed information about South Greenland sampling campaigns is provided in Weber et al. (2021).

2.2 Soil texture and organic matter content

The soil samples were first air-dried and passed through a 2-mm sieve. Then, the texture was measured with a combination of wet sieving and the pipette method after organic matter (OM) removal (Gee and Or, 2002). Further, total carbon was measured via high-temperature dry combustion with an ELTRA Helios C-Analyzer (ELTRA GmbH, Haan, NW, Germany). The soils did not test positive for calcium carbonate when 10% hydrochloric acid was used – hence, OC was assumed to be equal to total carbon. The measured OC content was converted to OM content using a conversion factor of 2 (Pribyl, 2010). For this work, clay, silt, and sand, and OM contents summed up to 100% on a mass basis.

2.3 Water vapor sorption isotherms

The WSIs of the investigated samples were determined on air-dry samples via adsorption and desorption for the relative humidity (*RH*) range from 3% to 93% (measurement resolution and temperature of 2% *RH* and 25°C, respectively). The measurements were conducted using an automated vapor sorption analyzer (METER Group Inc., Pullman, WA, USA). After the measurements, the samples were oven-dried for 48 h at 105°C to determine the water contents at the respective *RH* values. Further details about the measurement methodology are provided in Arthur et al. (2014).

The WSIs were used to characterize the water sorption of the soils using three sets of indices: (i) the water contents at the respective *RH* values, (ii) water sorption hysteresis, and (iii) the parameters of the Guggenheim, Anderson, and de Boer (GAB) model based on the van den Berg and Bruin (1981) isotherm equation that was developed by Anderson (1946), de Boer (1953) and Guggenheim (1966).

First, the *w* values for 18 selected *RH* values (10 to 90% with *RH* increments of 5%) were obtained directly from the adsorption and desorption data by linear interpolation between the two closest points. Second, the magnitude of hysteresis (*Hys*) was determined for the *RH* range from 10 to 80% using Equation 1 (Arthur et al., 2020):

$$Hys = \left[\left(\sum_{i=y}^{i=x} w_{\mathrm{d}} - w_{\mathrm{a}} \right) / n \right] \times 100 , \qquad (1)$$

where w_{d} and w_{a} are the water contents obtained via desorption and adsorption, respectively at a given point *i*, and *n* is the number of selected data points. Third, the GAB model was parameterized

with both the adsorption and desorption data for the *RH* range from 3% to 93%. The general form of the GAB equation is given as:

$$w = \frac{w_m \times C \times K \times RH}{\left[(1 - K \times RH)(1 - K \times RH + C \times RH)\right]}, \quad (2)$$

where w is water content (kg kg^{-1}), w_m (kg kg^{-1}) is the monolayer water content, C is an energy constant, and K represents the difference of free enthalpy of the water molecules in the pure liquid and the layers above the monolayer, RH is the relative humidity (%). The GAB equation was parameterized with the measured data by using the Levenberg–Marquardt nonlinear least squares algorithm implemented in the 'minpack.lm' package in R v4.0.2 (R Development Core Team, 2020).

2.4 Soil water repellency

The molarity of an ethanol droplet (MED) test was applied to measure the magnitude of WR (de Jonge et al., 1999; Roy and McGill, 2002; Hermansen et al., 2019). The soil was added to a disposable sample cup, and a small putty knife was used to smoothen the sample surface. Then, a 120 g weight was placed on the soil surface for 2 minutes. Solutions of pure water and ethanol, in the concentration range between 0.00 and 0.80 m^3 m^{-3}, were used for the experiment. Three to seven droplets (60 µL) of varying water and ethanol solution concentrations were pipetted onto the smooth soil surface. The resulting magnitude of WR corresponded to the highest concentration of ethanol that remained on the soil surface after 5 s. The resulting concentration of ethanol was converted to the unit of surface tension (mN m^{-1}) (Roy and McGill, 2002).

The WR measurements were performed on soil samples with varying w between completely oven-dry conditions and w_{non}. For all soils, the w range across which the WR-w curves were measured exceeded the w range for which the WSIs were measured. Initially, air-dried and 2-mm sieved soil samples were subjected to different pretreatments to reach water contents below and above air-dry conditions. For the WR measurement on completely dry soils, the samples were oven-dried at 105°C for 24 h and subsequently cooled down in a desiccator. Further, measurements of WR were performed on soil samples, which were oven-dried at 60°C for 24 h and subsequently equilibrated at 20°C in a temperature-controlled laboratory for 48 h. To reach water-contents above air-dry, the initially air-dried soil samples were re-wetted via the addition of deionized water. The amount of water that was added to each sample was predetermined and soil-specific. After addition of water, the soils were equilibrated for at least two weeks in sealed plastic bags before WR measurements. After the WR measurements, the w was determined after oven drying of the samples at 105°C.

The WR_{area} was determined as the trapezoidal integrated area under the WR-w curve in the range of w between oven-dried conditions (105°C) and w_{non}, i.e., the water content at which WR ceased.

2.5 Modeling and statistical analyses

Prior to statistical analyses, the water sorption variables, water repellency variables, and the other soil properties were tested for normality (Shapiro–Wilk test) and homogeneity of variance (Brown Forsythe test). Thereafter, simple and multiple linear regressions (MLRs) including OC and clay contents for estimation of WSI and WR parameters were performed with SigmaPlot 11.0 (Systat Software, Inc, San Jose, CA, USA). Furthermore, the WR parameters (WR_{area} and w_{non}) were regressed

individually against *w* at 18 selected RH values between 10 and 90%, separately for adsorption and desorption. The regression equations were of the form:

$$WR_{area} = b_1 \times w_{RH} \quad (3)$$

$$w_{non} = b_2 \times w_{RH} \quad (4)$$

where b_1 and b_2 are the water content regression coefficients, and w_{RH} is the water content at arbitrary *RH*. After obtaining the 18 equations each for adsorption and desorption for WR_{area} and w_{non}, a polynomial function was used to relate the b_1 and b_2 values to *RH* to enable the estimation of b_1 and b_2 at an arbitrary *RH* value between 10 and 90%.

The correlation coefficient (r^{CV}) and root mean square error ($RMSE^{CV}$) of cross-validation were used as statistical indices for evaluating model performance.

3. Results & Discussion

3.1 Soil texture and organic carbon contents

The 32 soil samples from Denmark and South Greenland exhibited clay and OC contents ranging from 0.02 to 0.16 kg kg^{-1} and 0.014 to 0.369 kg kg^{-1}, respectively (Table 1). Thus, the samples used in this study represent soils, which in general have a high organic carbon content.

Table 1. Descriptive statistics of soil properties for the 32 investigated soil samples.

Property†	Units	Min	Max	Mean‡	Median	IQ1§	IQ3
Clay	kg kg^{-1}	0.02	0.16	0.06	0.06	0.04	0.08
Silt		0.03	0.35	0.16	0.13	0.06	0.25
Sand		0.03	0.92	0.47	0.51	0.24	0.70
OC		0.014	0.369	0.154	0.111	0.062	0.233
GAB−$w_{m\text{-}a}$	kg kg^{-1}	0.0032	0.0960	0.0363	0.0250	0.0156	0.0538
GAB−C_a		3.73	47.5	23.2	23.0	17.0	30.2
GAB−K_a		0.70	0.77	0.73	0.74	0.72	0.75
GAB−$w_{m\text{-}d}$		0.0061	0.152	0.0592	0.0398	0.0241	0.0940
GAB−C_d		6.24	26.3	18.2	19.3	14.3	21.9
GAB−K_d		0.50	0.60	0.56	0.55	0.54	0.59
w_{50a}		0.0036	0.1490	0.0559	0.0368	0.0225	0.0885
w_{50d}		0.0055	0.1920	0.0735	0.0490	0.0294	0.120
Hys		0.0017	0.0416	0.0163	0.0110	0.0062	0.0284
WR_{area}	mN m^{-1} kg kg^{-1}	0.50	42.8	14.50	11.30	4.90	23.20
w_{non}	kg kg^{-1}	0.030	1.73	0.52	0.40	0.20	0.71

†GAB−$w_{m\text{-}a}$ and GAB−$w_{m\text{-}d}$, monolayer water content for adsorption and desorption curves; GAB−C_a and GAB−C_d, energy constants for adsorption and desorption; GAB−K_a and GAB−K_d, additional model parameters for adsorption and desorption, respectively, representing the difference of free enthalpy of the water molecules in the pure liquid and the layers above the monolayer; w_{50a} and w_{50d}, water content at 50% RH for adsorption and desorption; *Hys*, sorption hysteresis for a RH range from 10 to 80%; WR_{area}, total degree of soil water repellency; w_{non}, critical soil-water content. ‡Arithmetic mean. §IQ1 and IQ3, first and third quartiles of the dataset.

3.2 Characterization of soil water vapor sorption

The WSIs in Fig. 1a illustrate adsorption-desorption isotherms for two soil samples with differing clay (0.11 and 0.16 kg kg^{-1}) and OC (0.23 and 0.32 kg kg^{-1}) contents. In general, the WSIs of the two samples as well as of the remaining samples exhibited a sigmoidal shape (Arthur et al., 2016) (Supplementary Figs. S1 and S2). Fig. 1a also depicts how the *w* at selected RH values (e.g., RH = 50%) were derived for both adsorption and desorption; w_{50a} and w_{50d} correspond to the soil *w* at 50% *RH* for adsorption and desorption, respectively. Considering all investigated samples, w_{50a} ranged from 0.0036 to 0.149 kg kg^{-1} and w_{50d} ranged from 0.0055 to 0.192 kg kg^{-1} (Table 1). The range of w_{50a} is comparable to the w_{50a} range obtained in a study by Arthur et al. (2021). The latter study used mineral soil samples from different countries and found that w_{50a} values ranged from 0.010 to 0.145 kg kg^{-1} for samples with clay contents ranging from 0.08 to 0.89 kg kg^{-1} and OC contents ranging from 0.00 to 0.047 kg kg^{-1}. However, the range of w_{50a} is significantly wider than what was observed in the study of Wuddivira et al. (2012), where w_{50a} ranged from 0.010 to 0.045 kg kg^{-1} for samples with clay contents from 0.01 to 0.82 kg kg^{-1}.

An illustration of sorption hysteresis and the *RH* range for which *Hys* was calculated in this study is depicted in Fig. 1a. All investigated samples exhibited significant water vapor sorption hysteresis ranging from 0.0017 to 0.0416 kg kg^{-1} with a mean value of 0.0163 kg kg^{-1} (Table 1). Compared to mineral soils, the samples in this study were markedly more hysteretic than 147 mineral samples of varying clay mineralogy (clay: 0.02 to 0.83 kg kg^{-1}, OC: 0.003 to 0.084 kg kg^{-1}) investigated by Arthur et al. (2020). From the above observations of water sorption and hysteretic behavior, we can infer that the organic matter rich samples considered here have higher water sorption capacity when compared to mineral soil samples. This is mainly due to the strong affinity of functional groups such as carboxylic, amino, and phenolic hydroxyl groups to water molecules (Hurraß, 2006). Large soil OC contents result in increased hysteresis, and Arthur et al. (2020) reported that for samples with the same clay content and mineralogy, hysteresis increased with increasing OC content due to the conformational changes in the functional hydrophilic and hydrophobic groups on the sorption sites. The study of Chen et al. (2018) induced water repellency to pure clay minerals (kaolinite and montmorillonite) by adding two hydrophobic compounds (either saturated by cetyl trimethylammonium bromide or mixed with stearic acid in different concentrations). For the montmorillonites, hysteresis decreased when water repellency was induced by both of these hydrophobic compounds. The composition of OM is complex, due to e.g. varying decomposition level and origin. Thus, the effect of soil OM on WSIs might not be directly comparable with the effect of cetyl trimethylammonium bromide and stearic acid.

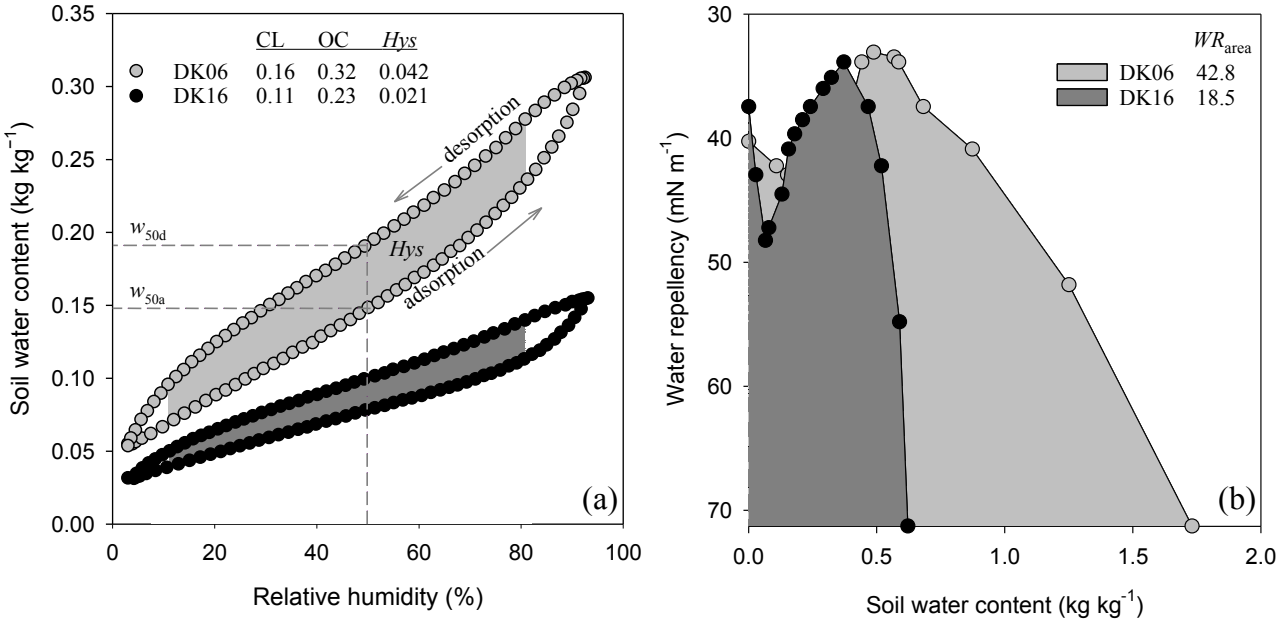

Figure 1. Comparison of (a) water vapor sorption isotherms and (b) soil water repellency (WR) as a function of gravimetric water content for two soil samples with differing clay (CL) and OC contents (kg kg^{-1}). The soil water contents at 50% relative humidity were derived for both adsorption (w_{50a}) and desorption (w_{50d}) isotherms. Sorption hysteresis (Hys in kg kg^{-1}) was derived based on the RH range from 10 to 80%. Total WR (WR_{area}) was determined as the trapezoidal integrated area below each curve.

The GAB model accurately captured the measured WSIs for all 32 samples for both adsorption and desorption isotherms. The model fit was characterized, on average, by low RMSE and high r^2 values for adsorption (RMSE of 0.0015 kg kg^{-1}; r^2 of 0.997) and desorption (RMSE of 0.0016 kg kg^{-1}; r^2 of 0.997).

The monolayer *w* parameter, obtained from the GAB model fit to the WSIs, varied between 0.0032 to 0.0960 kg kg^{-1} for adsorption curves ($w_{m\text{-}a}$) and 0.0061 to 0.152 kg kg^{-1} for desorption curves ($w_{m\text{-}d}$) (Table 1). The larger $w_{m\text{-}d}$ compared to $w_{m\text{-}a}$ corresponds to findings in Arthur et al. (2016) where $w_{m\text{-}a}$ ranged from 0.0014 to 0.063 kg kg^{-1} and $w_{m\text{-}d}$ ranged from 0.0021 to 0.089 kg kg^{-1} for soil samples representing a clay content range from 0.01 to 0.56 kg kg^{-1} and an OC content range from 0.001 to 0.022 kg kg^{-1}. Comparatively, the $w_{m\text{-}a}$ and $w_{m\text{-}d}$ values were larger in this study due to the increased water sorption capacity associated with the high OC contents of the samples.

The C parameter (Eq. 2) represents the binding strength of water to the primary sorption sites of the soil particles (Sabard et al., 2012), because it accounts for the difference in chemical potential between water molecules in the monolayer and the layers above the monolayer (multilayers). Thus, increasing C values represent increasing binding strength. In this study, the adsorption C (C_a) ranged from 3.73 to 47.5 kg kg^{-1} and desorption C (C_d) ranged from 6.24 to 26.3 kg kg^{-1}. The finding that C_a values were higher than C_d values is in accordance with the study of Arthur et al. (2016) (C_a range: 6 to 115; C_d range: 4 to 67). The reasoning for this difference in chemical potential between adsorption and desorption processes is that the binding energy is higher during adsorption, despite fewer available sorption sites (Arthur et al., 2016).

The K parameter (Eq. 2) represents the interactions of water molecules contained in the multilayers with the soil particles, because it accounts for the relative differences in free enthalpy of water molecules in the multilayer and bulk liquid (Arthur et al., 2016). Hence, a higher K value represents an increased attraction of water molecules in the multilayer to the soil particle surfaces. The K_a ranged from 0.70 to 0.77 kg kg^{-1} and the K_d ranged from 0.50 to 0.60 kg kg^{-1}. The K values were higher for the adsorption than for the desorption isotherms, implying a stronger interaction between the soil particle surfaces and water molecules in the multilayer during adsorption. Higher values of K_a and K_d were found in the study of Arthur et al. (2016) (K_a range: 0.53 to 0.93 kg kg^{-1}; K_d range: 0.43 to 0.87 kg kg^{-1}). For soils where the clay content exceeds the OM content, it is generally assumed that the clay fraction acts as the primary sorbent (Arthur et al., 2016). However, the soils in this study exhibit high OC contents, and therefore, the OC fraction has a significant impact on the attraction of water molecules in the multilayer to the soil particle surfaces.

Table 2. Models for water vapor sorption (WSI) variables based on either organic carbon (OC) in a linear regression or OC and clay (CL) in a multiple linear regression. The models were based on the 32 investigated soil samples.

WSI variable† (kg kg^{-1})	Equation; x_1 = OC (kg kg^{-1}), x_2 = CL (kg kg^{-1})‡	r^2_{adj}	RMSE^{CV}§ (×10^{-2})	r^{CV}¶
$w_{m\text{-}a}$	$y = 0.24\ x_1$	0.98	0.68	0.97
	$y = 0.22\ x_1 + 0.12\ x_2 - 0.54$	0.95	0.61	0.98
$w_{m\text{-}d}$	$y = 0.39\ x_1$	0.98	1.11	0.97
	$y = 0.36\ x_1 + 0.18\ x_2 - 0.74$	0.95	1.04	0.97
w_{50a}	$y = 0.37\ x_1$	0.98	1.11	0.97
	$y = 0.34\ x_1 + 0.21\ x_2 - 0.97$	0.94	1.00	0.97
w_{50d}	$y = 0.48\ x_1$	0.97	1.50	0.97
	$y = 0.44\ x_1 + 0.26\ x_2 - 1.18$	0.94	1.37	0.97
Hys	$y = 0.11\ x_1$	0.96	0.42	0.95
	$y = 0.10\ x_1 + 0.06\ x_2 - 0.24$	0.90	0.40	0.95

†$w_{m\text{-}a}$, adsorption monolayer water content; $w_{m\text{-}d}$, desorption monolayer water content; w_{50a}: water content at 50% relative humidity for adsorption; w_{50d}, water content at 50% relative humidity for desorption; *Hys*, hysteresis (10 – 80% relative humidity). ‡r^2_{adj}, adjusted coefficient of determination from linear- or multiple linear regression. §RMSE^{CV}: root mean square error from cross-validation. ¶r^{CV}, correlation coefficient from cross-validation.

Based on visual inspection of the measured WSIs sorted from lowest to highest OC content (Fig. 2; Supplemental Figs. S1 and S2), water sorption at any given *RH* increases with increasing OC content. The hysteresis effect seems higher at higher OC contents. Consequently, we examined the potential of using clay and OC contents for the estimation of the five WSI variables ($w_{m\text{-}a}$, $w_{m\text{-}d}$, w_{50a}, w_{50d}, and *Hys*). From Table 2 it is obvious that both using only OC or OC in combination with clay content, well estimated all WSI variables (r^2_{adj} between 0.90 and 0.98). When comparing the model performance of linear OC models with the MLRs based on OC and clay contents, the addition of clay content for estimation of WSI parameters resulted in slightly lower RMSE^{CV} values for all parameters. In the MLRs, OC content contributed significantly ($p < 0.001$) to the estimation of all WSI parameters, while clay content contributed significantly only to the stimation of $w_{m\text{-}a}$, w_{50a}, and w_{50d} ($p < 0.05$). Furthermore, there was no clear differentiation based on sample origin (Greenland or Obakker in Denmark) in the trend of the relationship between OC and the WSI variables (Fig. 3).

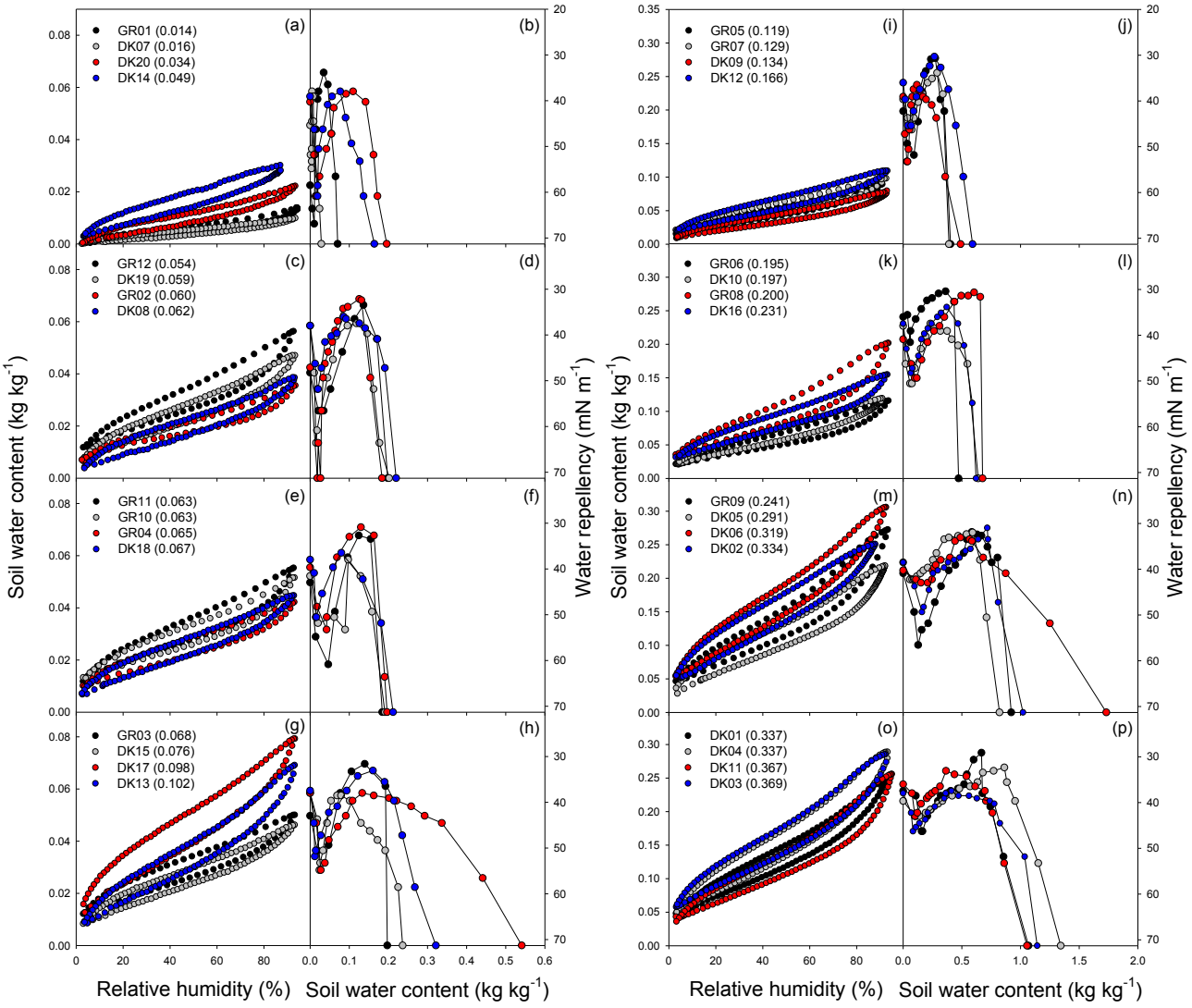

Figure 2. Water vapor sorption isotherms (a, c, e, g, l, k, m, and o) and soil water repellency versus water content curves (b, d, f, h, j, l, n, and p) for the 32 soil samples from Denmark (DK01 – DK20) and Greenland (GL01 – GL12) sorted from the lowest to highest OC contents (given in kg kg^{-1} for each soil in the brackets). Note the difference in the scale of the soil water content x-axis between the left and right panels.

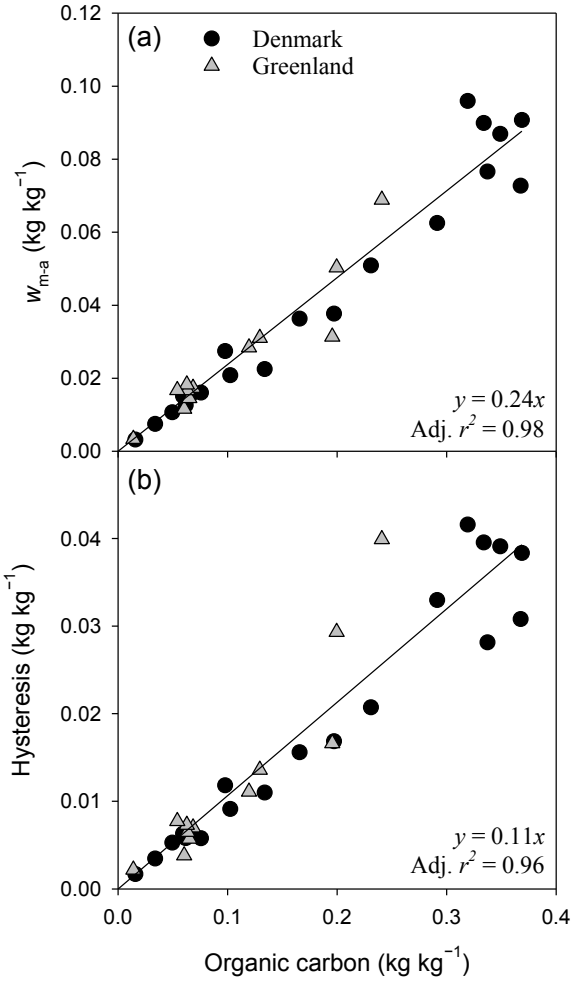

Figure 3. a) The adsorption monolayer water content derived from the Guggenheim, Anderson, and de Boer model and b) hysteresis as a function of OC content.

3.3 Characterization of the soil water repellency curves

The WR-*w* curves of sample DK06 (high clay and OC contents) and DK16 (low clay and OC contents) are depicted in Fig. 1b. Both soils exhibit a bimodal behavior, with a local decrease in WR around air-dry conditions (de Jonge et al., 1999; Regalado et al., 2008). The trapezoidal integrated area (WR_{area}) under the WR-*w* curve of DK06 (42.8 mN m^{-1} kg kg^{-1}) was higher than the WR_{area} of DK16 (18.5 mN m^{-1} kg kg^{-1}). The *w* at which WR ceased (w_{non}) was also higher for DK06 (1.73 kg kg^{-1}) than for DK16 (0.62 kg kg^{-1}). This difference is caused by the difference in OC content between the samples since WR_{area} and w_{non} generally increase with OC content (Hermansen et al., 2019; Weber et al., 2021). For the entire dataset, WR_{area} ranged from 0.50 to 42.8 mN m^{-1} kg kg^{-1} and w_{non} from 0.030 to 1.73 kg kg^{-1}. For comparison, the range of WR_{area} was 0.16 to 26.82 mN m^{-1} kg kg^{-1} and the range of w_{non} was 0.07 to 0.78 kg kg^{-1} in the study of Hermansen et al. (2019). Thus, the ranges of WR_{area} and w_{non} were lower in the study by Hermansen et al. (2019), which included soil samples with clay contents ranging from 0.00 to 0.52 kg kg^{-1} and OC contents ranging from 0.021 to 0.217 kg kg^{-1}.

Table 3. Comparison of models for the trapezoidal integrated area below the soil water repellency versus water content curve (WR_{area}) and the critical water content (w_{non}). Models consist of linear

regressions using OC (kg kg^{-1}) and water vapor sorption parameters as estimation variables or multiple linear regressions using a combination of OC and clay (CL, kg kg^{-1})

WR parameter (*y*)	Equation‡	r^2_{adj}	RMSE^{CV}§	r^{CV}¶
WR_{area} (mN m^{-1} kg kg^{-1})	$y = 95 \times OC$	0.97	3.12	0.96
	$y = 83 \times OC + 74 \times CL - 299$	0.94	2.65	0.97
	$y = 397 \times w_{m\text{-}a}$	0.98	2.46	0.95
	$y = 244 \times w_{m\text{-}d}$	0.98	2.52	0.95
	$y = 256 \times w_{50a}$	0.98	2.46	0.95
	$y = 195 \times w_{50d}$	0.98	2.48	0.95
	$y = 873 \times Hys$	0.97	3.06	0.93
w_{non} (kg kg^{-1})	$y = 3.4 \times OC$	0.95	0.145	0.94
	$y = 2.7 \times OC + 3.6 \times CL - 12$	0.91	0.122	0.96
	$y = 14.3 \times w_{m\text{-}a}$	0.97	0.105	0.97
	$y = 8.75 \times w_{m\text{-}d}$	0.97	0.115	0.96
	$y = 9.20 \times w_{50a}$	0.97	0.110	0.96
	$y = 7.00 \times w_{50d}$	0.97	0.114	0.96
	$y = 31.3 \times Hys$	0.96	0.138	0.94

†$w_{m\text{-}a}$, adsorption monolayer water content; $w_{m\text{-}d}$, desorption monolayer water content; w_{50a}: water content at 50% relative humidity for adsorption; w_{50d}, water content at 50% relative humidity for desorption; *Hys*, hysteresis (10 – 80% relative humidity). ‡r^2_{adj}, adjusted coefficient of determination from linear- or multiple linear regression.
§RMSE^{CV}, root mean square error from cross-validation.
¶r^{CV}, correlation coefficient from cross-validation.

With regard to the WR-*w* curves depicted in Fig. 2, the area below the curves increased with increasing OC content (Supplemental Figs. S3 and S4). All samples reached an extreme degree of WR, according to the definition by Doerr et al. (2000) (extreme WR > 20% ethanol, corresponding to 40.88 mN m^{-1}). For this dataset, WR_{area} and w_{non} increased linearly as a function of OC content (r^2_{adj} of 0.97 and 0.95) (Table 3 and Fig. 4a and b), which conforms to findings of previous studies (Kawamoto et al., 2007; Regalado et al., 2008; Hermansen et al., 2019; Weber et al., 2021). The inclusion of clay and OC content in an MLR for estimation of WR_{area} and w_{non} resulted in lower RMSE^{CV} values (RMSE^{CV} of 2.65 mN m^{-1} kg kg^{-1} and 0.122 kg kg^{-1}) than for the estimation of WR_{area} and w_{non} with the linear regressions based on OC content (RMSE^{CV} of 3.12 mN m^{-1} kg kg^{-1} and 0.145 kg kg^{-1}) (Table 3). For the MLRs, both OC content and clay content significantly contributed to the estimations ($p < 0.001$ and $p < 0.05$). In comparison, the study of Hermansen et al. (2019) obtained RMSE^{CV} values of 2.09 mN m^{-1} kg kg^{-1} and 0.062 kg kg^{-1} from linear regressions for WR_{area} and w_{non} with only OC as estimation variable. However, this study did not find a significant contribution of clay content to explain variations in WR_{area} and w_{non}. Yet, the study of Weber et al. (2021) found clay content to contribute to a more accurate estimation of w_{non} in an MLR including both OC and clay contents.

3.4 Linking WSIs and WR-w curves and the potential for estimating water repellency from water sorption

The water sorption at any given *RH* as well as WR_{area} both increased with increasing OC content (Fig. 2). The theoretical explanation for the causes of WR and the hysteretic behavior of water vapor sorption is somewhat similar. The contribution of OC to both WR and the hysteresis effect might be related to the conformational changes in the orientation of hydrophobic and hydrophilic functional

groups of OM (Doerr et al., 2000; Arthur et al., 2020). The hydrophilic groups of organic matter (hydroxyl, amide, carboxylate, and carboxylic acid) have an affinity for water molecules, but in dry soils these functional groups interact and expose nonpolar fractions of OM, causing the soil to be hydrophobic (Ma'shum et al., 1988; Doerr et al., 2000). Further, the orientation of hydrophilic functional groups in OM, and thereby available sorption sites for water molecules, during adsorption and desorption is not similar, which result in hysteresis (Arthur et al., 2020). It is therefore possible that, in soils with high OC contents as investigated here, the two processes (water sorption and water repellency) are interlinked. We, therefore, investigated the potential of using the WSI variables as estimates for the water repellency variables.

We found that the WSI parameters ($w_{m\text{-}a}$, $w_{m\text{-}d}$, w_{50a}, w_{50d}, and *Hys*) were all highly linearly correlated to both WR_{area} (r^2_{adj} from 0.97 to 0.98) and w_{non} (r^2_{adj} from 0.96 to 0.97) (Fig. 4c to f). In cross-validation, the lowest $RMSE^{CV}$ for WR_{area} was obtained with the models based on $w_{m\text{-}a}$ and w_{50a} ($RMSE^{CV}$ 2.46 mN m^{-1} kg kg^{-1} for both), and the lowest $RMSE^{CV}$ for w_{non} was obtained with the model based on $w_{m\text{-}a}$ ($RMSE^{CV}$ 0.105 kg kg^{-1} for both). For these samples, the OC content is the probable driver for successful estimation of WR parameters from WSIs, although it may seem contradictory that the OC content in these soils is both the driver of the high water vapor sorption and the high severity of WR. As previously noted, the severity of WR tends to increase with increasing OC content (de Jonge et al., 1999; Hermansen et al., 2019; Weber et al., 2021). For standard soils (soils that have < 0.02 kg kg^{-1} OC), the clay and silt fractions determine the magnitude of water vapor sorption (Arthur et al., 2015). However, the soils in this study have very high OC contents (up to 0.369 kg kg^{-1}), which means that OC becomes the driver of water vapor sorption. Thus, for these specific soils, OC can link water vapor sorption and WR, because OC drives the two processes in the same direction.

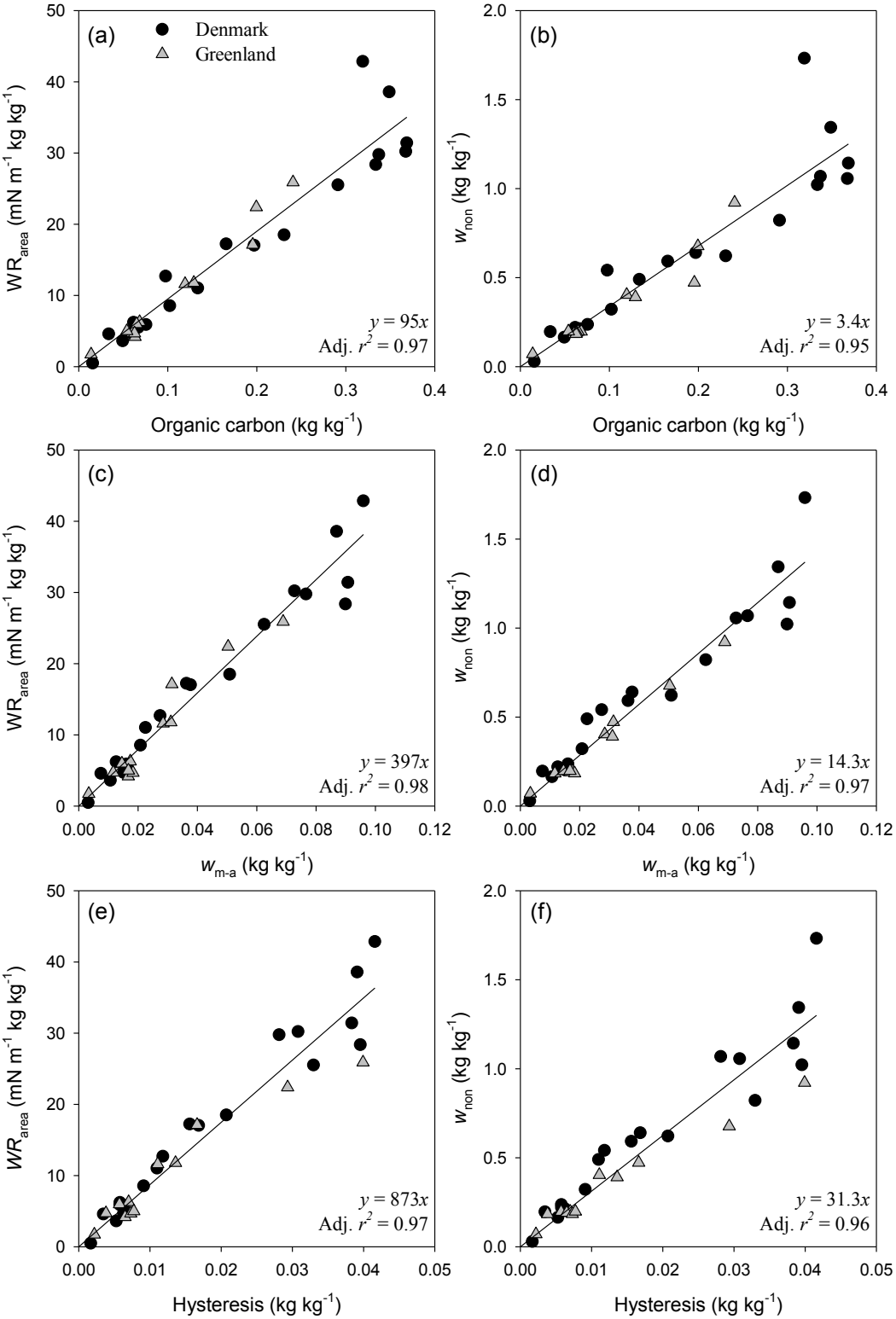

Figure 4. Total soil water repellency (WR_{area}) (a, c, and e) and critical water content (w_{non}) (b, d, and f) as a function OC, the monolayer water content derived from the Guggenheim, Anderson, and de Boer model for adsorption isotherms ($w_{m\text{-}a}$), and water sorption hysteresis.

Further, we were able to combine Danish and Greenlandic soil samples into one dataset, for which WR-*w* curve parameters (WR_{area} and w_{non}) plotted as a function of OC followed the same slope. This

suggests that the two sites had similar SOM composition. The study of Weber et al. (2021) also combined soil samples from Greenland and New Zealand and found that WR followed an almost identical trend when plotted as a function of OC.

For practical application of the equations in Table 3 one will require either the full WSI (to estimate *Hys* and the GAB parameters) or *w* measured at a fixed *RH* of 50%. In the majority of cases, where WR variables have to be estimated for several samples within a short period of time, it remains a practical limitation to measure the full WSI or ensure an *RH* of 50%. It would be favorable if WR_{area} and w_{non} could be derived from a simple water content measurement regardless of *RH*. To address this challenge, the polynomial functions for computing the water content coefficient (*b*) values for estimating WR_{area} and w_{non} are presented in Fig. 5. To use the model, one only has to equilibrate the sample at a known *RH* to obtain *w,* select the appropriate polynomial function (considering the sorption direction and *RH*), compute the regression coefficient and multiply it with the *w* value. The only prerequisites for application of this approach is a RH sensor and a laboratory oven to determine *w*. This procedure represents a rapid and easy approach to estimate WR_{area} and w_{non} from water content.

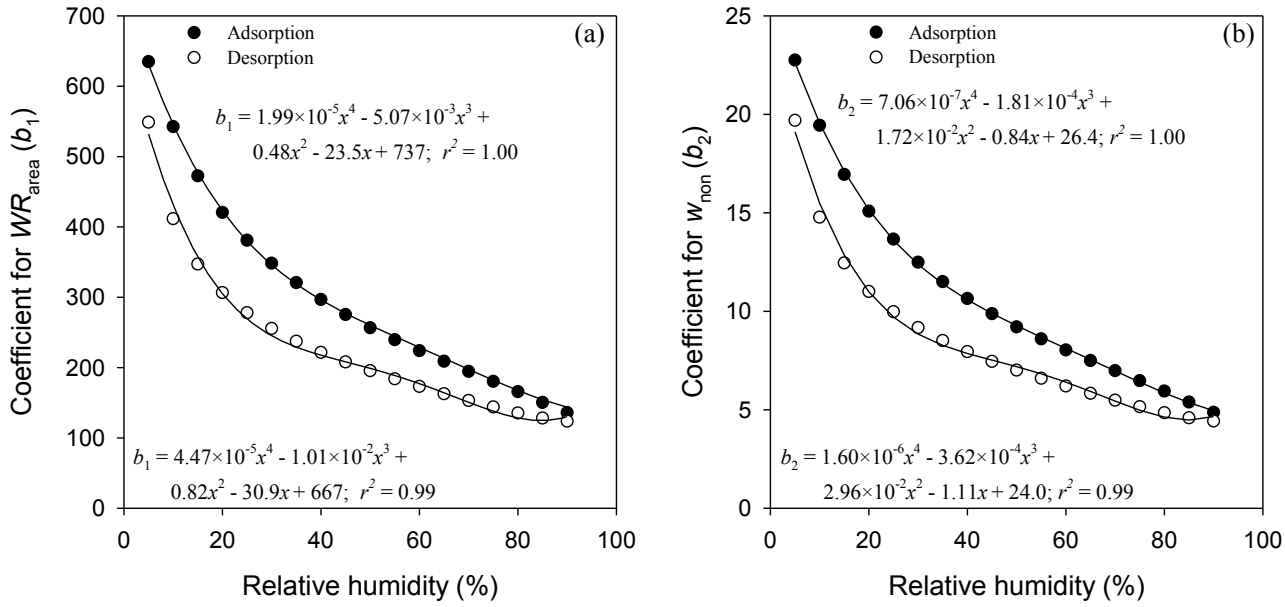

Figure 5. Coefficients for determining (a) the total soil water repellency, WR_{area}, and (b) critical water content (w_{non}) from relative humidity (RH) for both adsorption and desorption data. In the equations, x represents the relative humidity (%).

4. Conclusions

In this study, we investigated the links between soil composition, water vapor sorption isotherms (WSIs), and soil water repellency (WR) for 32 organic matter rich soil samples (OC between 0.014 and 0.369 kg kg^{-1}) from Denmark and South Greenland.

We found that parameters derived from the water vapor sorption isotherms ($w_{m\text{-}a}$, $w_{m\text{-}d}$, w_{50a}, w_{50d}, and *Hys*) were linearly correlated to OC content, and inclusion of clay content (significant for the prediction of $w_{m\text{-}a}$, w_{50a}, and w_{50d}) in an MLR for WSI parameters slightly increased the performance.

We further observed a linear correlation between WR parameters (WR_{area} and $w_{non)}$ and OC content. Clay content had a significant and marginal positive effect on the estimation of WR parameters in an MLR including OC and clay. However, the models for WR_{area} and w_{non} based on the WSI parameters $w_{m\text{-}a}$, $w_{m\text{-}d}$, w_{50a}, and w_{50d} had the lowest errors. Based on the interrelation between WR parameters, WSI parameters, and soil composition (i.e., OC and clay contents), it was obvious that OC content was the driving link between WSI and WR parameters for all investigated samples.

Lastly, we were able to establish mathematical expressions to obtain WR_{area} and w_{non} from water contents measured at any relative humidity between 10 and 90 % for both water vapor adsorption and desorption. This significantly increases the practical applicability of the water content-based models, as it circumvents the need for advanced laboratory equipment.

Although the number of samples for this study was limited, we found that the two groups of soils collected in different geographic regions and under varying climatic conditions could be merged into one group for the purpose of model development for WSI and WR parameters. This suggests that the relations we found between texture, OC, WSI parameters and WR parameters are universal for the studied soils. Thus, it will be interesting to test this hypothesis on soil from other world regions.

Acknowledgements

This study was funded by the VILLUM FONDEN research grant 13162 and the Danish Council for Independent Research, Technology, and Production Sciences via the project “Glacial Flour as a New, Climate-Positive Technology for Sustainable Agriculture in Greenland: NewLand” (Grant number: 8022-00184B). Co-author Markus Tuller acknowledges support from United States Department of Agriculture (USDA) National Institute of Food and Agriculture (NIFA) Hatch/Multi-State project number ARZT-1370600-R21-189.

Conflict of interest

The authors declare no conflict of interest.

Supplemental Material

Please find Supporting Figures online. Supplementary Figure S1 and S2 depict water vapor sorption isotherms, and Supplementary Figure S3 and S4 depict soil water repellency versus water content curves for the Danish and Greenlandic soil samples.

References

Anderson, R.B. 1946. Modifications of the Brunauer, Emmett and Teller Equation. J. Am. Chem. Soc. 68:686-691. doi:10.1021/ja01208a049

Arthur, E., M. Tuller, P. Moldrup, and L.W. de Jonge. 2014. Rapid and fully automated measurement of water vapor sorption isotherms: New opportunities for vadose zone research. Vadose Zone J. 13. doi:10.2136/vzj2013.10.0185

Arthur, E., M. Tuller, P. Moldrup, and L.W. de Jonge. 2016. Evaluation of theoretical and empirical water vapor sorption isotherm models for soils. Water Resour. Res. 52:190-205. doi:10.1002/2015wr017681

Arthur, E., M. Tuller, P. Moldrup, and L.W. de Jonge. 2020. Clay content and mineralogy, organic carbon and cation exchange capacity affect water vapour sorption hysteresis of soil. Eur. J. Soil Sci. 71:204-214. doi:10.1111/ejss.12853

Arthur, E., M. Tuller, P. Moldrup, D.K. Jensen, and L.W. de Jonge. 2015. Prediction of clay content from water vapour sorption isotherms considering hysteresis and soil organic matter content. Eur. J. Soil Sci. 66:206-217. doi:10.1111/ejss.12191

Arthur, E., H.U. Rehman, M. Tuller, N. Pouladi, T. Nørgaard, P. Moldrup, and L.W. de Jonge. 2021. Estimating Atterberg limits of soils from hydroscopic water content. Geoderma 381, 1146198. doi:10.1016/j.geoderma.2020.114698

Chen, J.J., K.J. McGuire, and R.D. Stewart. 2020. Effect of soil water-repellent layer depth on post-wildfire hydrological processes. Hydrol. Processes 34:270-283. doi:10.1002/hyp.13583

Chen, J.J., C. Shang, M.J. Eick, and R.D. Stewart. 2018. Water repellency decreases vapor sorption of clay minerals. Water Resour. Res. 54:6114-6125. doi:10.1029/2018wr023352

Davis, D.D., R. Horton, J.L. Heitman, and T.S. Ren. 2009. Wettability and hysteresis effects on water sorption in relatively dry soil. Soil Sci. Soc. Am. J. 73:1947-1951. doi:10.2136/sssaj2009.00028N

de Boer, J.H. 1953. The dynamical character of adsorption. Oxford University Press, Oxford.

de Jonge, L.W., O.H. Jacobsen, and P. Moldrup. 1999. Soil water repellency: Effects of water content, temperature, and particle size. Soil Sci. Soc. Am. J. 63:437-442. doi:10.2136/sssaj1999.03615995006300030003x

de Jonge, L.W., P. Moldrup, and O.H. Jacobsen. 2007. Soil-water content dependency of water repellency in soils: Effect of crop type, soil management, and physical-chemical parameters. Soil Sci. 172:577-588. doi:10.1097/SS.06013e318065c090

de Jonge, L.W., P. Moldrup, and P. Schjonning. 2009. Soil infrastructure, interfaces & translocation processes in inner space ('soil-it-is'): Towards a road map for the constraints and crossroads of soil architecture and biophysical processes. Hydrol. Earth Syst. Sci. 13:1485-1502. doi:10.5194/hess-13-1485-2009

DeBano, L.F. 1981. Water repellent soils: A state-of-the-art. USDA Forest Service General Technical Report PSW-46, 21pp.

Deurer, M., K. Müller, C. Van den Dijssel, K. Mason, J. Carter, and B.E. Clothier. 2011. Is soil water repellency a function of soil order and proneness to drought? A survey of soils under pasture in the North Island of New Zealand. Eur. J. Soil Sci. 62:765-779. doi:10.1111/j.1365-2389.2011.01392.x

Doerr, S.H., R.A. Shakesby, and R.P.D. Walsh. 2000. Soil water repellency: its causes, characteristics and hydro-geomorphological significance. Earth-Sci. Rev. 51:33-65. doi:10.1016/S0012-8252(00)00011-8

Gao, Y.F., H.L. Liu, H.X. Wu, and Alamus. 2018. Seasonal changes in soil water repellency of different land use types in Inner Mongolia grassland. Soil & Tillage Research 177:37-44. doi:10.1016/j.still.2017.11.011

Gee, G.W., and D. Or. 2002. Particle-size analysis. In: J.H. Dane and G.C. Topp, editors, Methods of Soil Analysis: Part 4. SSSA Book Ser. 5. SSSA, Madison, WI.

Guggenheim, E. 1966. Application of statistical mechanics. Oxford University Press, Oxford.

Harper, R.J., and R.J. Gilkes. 1994. Soil attributes related to water repellency and the utility of soil survey for predicting its occurrence. Aust. J. Soil Res. 32:1109-1124. doi:10.1071/Sr9941109

Hermansen, C., P. Moldrup, K. Müller, P.W. Jensen, C. Van den Dijssel, P. Jeyakumar, and L.W. de Jonge. 2019. Organic carbon content controls the severity of water repellency and the critical moisture level across New Zealand pasture soils. Geoderma 338:281-290. doi:10.1016/j.geoderma.2018.12.007

Hurraß, J. 2006. Hurraß, J., 2006. Interactions between soil organic matter and water with special respect to the glass transition behavior, Technische Universität Berlin. Doctoral Thesis. https://www.depositonce.tu-berlin.de/handle/11303/1633, 137 pp.

Karunarathna, A.K., K. Kawamoto, P. Moldrup, L.W. de Jonge, and T. Komatsu. 2010. A simple beta-function model for soil-water repellency as a function of water and organic carbon contents. Soil Sci. 175:461-468. doi:10.1097/SS.0b013e3181f55ab6

Kawamoto, K., P. Moldrup, T. Komatsu, L.W. de Jonge, and M. Oda. 2007. Water repellency of aggregate size fractions of a volcanic ash soil. Soil Sci. Soc. Am. J. 71:1658-1666. doi:10.2136/sssaj2006.0284

Leighton-Boyce, G., S.H. Doerr, R.A. Shakesby, and R.P.D. Walsh. 2007. Quantifying the impact of soil water repellency on overland flow generation and erosion: a new approach using rainfall simulation and wetting agent on in situ soil. Hydrol. Processes 21:2337-2345. doi:10.1002/hyp.6744

Ma'shum, M., M.E. Tate, G.P. Jones, and J.M. Oades. 1988. Extraction and characterization of water-repellent materials from Australian soils. J. Soil Sci. 39:99-110. doi:10.1111/j.1365-2389.1988.tb01198.x

Mas'shum, M., and V.C. Farmer. 1985. Origin and assessment of water repellency of a sandy South Australian soil. Aust. J. Soil Res. 23:623-626. doi:10.1071/SR9850623

Müller, K., M. Deurer, M. Slay, T. Aslam, J.A. Carter, and B.E. Clothier. 2010. Environmental and economic consequences of soil water repellency under pasture. Proc. N. Z. Grassl. Assoc. 72:207-210.

Osborn, J.F., R.E. Pelishek, J.S. Krammes, and J. Letley. 1964. Soil wettability as a factor in erodibility. Soil Sci. Soc. Am. J. 28:294-295. doi:10.2136/sssaj1964.03615995002800020050x

Pribyl, D.W. 2010. A critical review of the conventional SOC to SOM conversion factor. Geoderma 156:75-83. doi:10.1016/j.geoderma.2010.02.003

R Development Core Team. 2020. A language and environment for statistical computing. R Foundation for Statistical Computing, Vienna, Austria. URL http://www.R-project.org/.

Regalado, C.M., A. Ritter, L.W. de Jonge, K. Kawamoto, T. Komatsu, and P. Moldrup. 2008. Useful soil-water repellency indices: Linear correlations. Soil Sci. 173:747-757. doi:10.1097/SS.0b013e31818d4163

Roy, J.L., and W.B. McGill. 2002. Assessing soil water repellency using the molarity of ethanol droplet (MED) test. Soil Sci. 167:83-97. doi:10.1097/00010694-200202000-00001

Ruwanza, S., and C.M. Shackleton. 2016. Effects of the invasive shrub, Lantana camara, on soil properties in the Eastern Cape, South Africa. Weed Biol. Manage. 16:67-79. doi:10.1111/wbm.12094

Sabard, M., F. Guanvé, E. Espuche, R. Fulchiron, G. Seytre, L.A. Fillot, and L.T. Fonti. 2012. Influence of film processing conditions on the morphology of polyamide 6: Consequences on water and ethanol sorption properties. J. Membr. Sci. 415-416:670-680. doi:10.1016/j.memsci.2012.05.048

Scott, D.F. 2000. Soil wettability in forested catchments in South Africa; as measured by different methods and as affected by vegetation cover and soil characteristics. Journal of Hydrology 231-232:87-104. doi:10.1016/S0022-1694(00)00186-4

Seaton, F.M., D.L. Jones, S. Creer, P.B.L. George, S.M. Smart, I. Lebron, G. Barrett, B.A. Emmett, and D.A. Robinson. 2019. Plant and soil communities are associated with the response of soil

water repellency to environmental stress. Science of the Total Environment 687:929-938. doi:10.1016/j.scitotenv.2019.06.052

Tuller, M., and D. Or. 2005. Water films and scaling of soil characteristic curves at low water contents. Water Resour. Res. 41. doi:10.1029/2005wr004142

van den Berg, C., and S. Bruin. 1981. Water activity and its estimation in food systems. In: Water activity: influences on food quality (eds. Rockland, L.B. & Stewart, G.F.), pp. 147–177, New York: Academic Press.

Weber, P.L., C. Hermansen, T. Norgaard, C. Pesch, P. Moldrup, M.H. Greve, K. Müller, E. Arthur, and L.W. de Jonge. 2021. On the water repellency of Greenlandic cultivated soils. Submitted to Geoderma.

Wuddivira, M.N., D.A. Robinson, I. Lebron, L. Brechet, M. Atwell, S. De Caires, M. Oatham, S.B. Jones, H. Abdu, A.K. Verma, and M. Tuller. 2012. Estimation of soil clay content from hygroscopic water content measurements. Soil Sci. Soc. Am. J. 76:1529-1535. doi:10.2136/sssaj2012.0034